1,3-Dipolar cycloaddition reactions to the C:XM fragment. 7. The reaction of Ru(CO)3(iso-Pr-DAB) with dimethyl acetylenedicarboxylate. X-ray crystal structure of the protonated initial bicyclo[2.2.1] adduct

Maarten Van Wijnkoop, Paul P. M. De Lange, Hans Werner Fruhauf, Kees Vrieze, Yuanfang Wang, Kees Goubitz, and Casper H. Stam

Organometallics, **1992**, 11 (11), 3607-3617• DOI: 10.1021/om00059a025 • Publication Date (Web): 01 May 2002

Grant No. DMR 87-01968) for support, to the University of Konstanz for a guest professorship for T.J.K., to Professor Gerard Parkin for analyzing the structures of 13 and 22 by X-ray diffraction, and to Professor Gu Min-Min for her help in early stages of the work.

Note added in proof: Since this paper was submitted, we have synthesized four analogues of 17 and 18: those in which the methyls of the 3,4-dimethylcyclopentadienyls are replaced by tetramethylenes (yielding "**2-tetrahydroindenyls**") and those in which the biphenyls are replaced by **binaphthyls**. We intend to describe these shortly.

Supplementary Material Available: Listings of NOE and COSY data for 11, X-ray diffraction data for 17, 18, and 22, including tables of crystal data and refinement details, positional parameters, bond distances and angles, and thermal parameters, and a packing diagram for 22 (28 pages). Ordering information is given on any current masthead page.

OM920254W

1,3-Dipolar Cycloaddition Reactions to the C=X–M Fragment. 7. Reaction of $Ru(CO)_3$(*i*-Pr-DAB) with Dimethyl Acetylenedicarboxylate. X-ray Crystal Structure of the Protonated Initial Bicyclo[2.2.1] Adduct

Maarten van Wijnkoop, Paul P. M. de Lange, Hans-Werner Frühauf,* and Kees Vrieze

Laboratorium voor Anorganische Chemie, J. H. van't Hoff Instituut, Universiteit van Amsterdam, Nieuwe Achtergracht 166, 1018 WV Amsterdam, The Netherlands

Yuanfang Wang, Kees Goubitz, and Casper H. Stam

Laboratorium voor Kristallografie, J. H. van't Hoff Instituut, Universiteit van Amsterdam, Nieuwe Achtergracht 166, 1018 WV Amsterdam, The Netherlands

Received March 27, 1992

In situ prepared $Ru(CO)_3$(*i*-Pr-DAB) reacts instantly at −78 °C with 1 equiv of dimethyl acetylenedicarboxylate. When the reaction mixture is allowed to warm up to room temperature different bicyclic products are obtained, depending on the additional ligand offered. Under 1.1 atm of CO the ruthenabicyclo[2.2.2] complex **9a** can be isolated, which is spectroscopically characterized (IR and ^1H and ^{13}C NMR). This complex does not thermally rearrange to a 1,5-dihydropyrrol-2-one complex **5** as the analogous Fe complexes do, not even at elevated temperatures. When PPh_3 is used instead of CO, the PPh_3-substituted ruthenabicyclo[2.2.2] complex **9b** is formed which has been characterized by an X-ray structure determination. Crystals of **9b**, $C_{35}H_{37}N_2O_7PRu$, are orthorhombic, space group *Pnca*, with cell constants a = 18.699 (1) Å, b = 34.331 (2) Å, c = 11.530 (1) Å, V = 7401.7 Å^3, Z = 8, R = 0.031 (R_w = 0.061) for 5193 reflections with $I > 2.5\sigma(I)$. Addition of HBF_4, at low temperature, immediately after the cycloaddition results in formation of the ruthenabicyclo[2.2.1] complex **10**, $C_{17}H_{23}N_2O_7Ru^+BF_4^-$, of which the structure has been determined by single-crystal X-ray diffraction: crystals of **10** are orthorhombic, space group *Pbca*, a = 13.5335 (8) Å, b = 17.088 (1) Å, c = 20.645 (2) Å, V = 4774.4 (6) Å^3, Z = 8, R = 0.040 (R_w = 0.061) for 3634 reflections with $I > 2.5\sigma(I)$. In complex **10**, the former imine N atom is protonated which prevents the nucleophilic attack of this N-atom on a terminal CO ligand and hence the initial [2.2.1] bicyclic structure is retained. Reaction of $Ru(CO)_3$(*i*-Pr-DAB) with excess DMADC in the absence of an additional ligand results in the formation of (1,4,3a,6a-tetrahydropyrrolo[3,2-*b*]pyrrole)$Ru(CO)_3$ (**11**). The newly formed heterocyclic ligand is readily displaced from the complex at slightly elevated temperature.

Introduction

In earlier papers we have reported the reactions of (1,4-diaza-1,3-butadiene)tricarbonyliron complexes $Fe(CO)_3$(R-DAB)[1] with electron-deficient alkynes following the reaction sequence shown in Scheme I and finally resulting in the formation of (1,5-dihydropyrrol-2-one)tricarbonyliron complexes (**4**).[2-6] The bicyclo[2.2.2] complex (**3**) was the first intermediate that could be isolated and fully characterized. The initial step in which the electron-deficient alkyne reacts with $Fe(CO)_3$(R-DAB) to form the intermediate [2.2.1] bicyclic compound **2** has been described in terms of an oxidative 1,3-dipolar [3 + 2] cycloaddition. This proposal was supported by the fact that is was possible to isolate and characterize a bicyclo[2.2.1] complex (Figure 1)[6] closely resembling the initial cyclo-

* To whom correspondence should be addressed.

(1) The abbreviations used throughout this text are as follows. The 1,4-diaza 1,3-dienes of formula RN=C(H)C(H)=NR are abbreviated as R-DAB. R-ADA stands for 1,6-di-R-1,6-diazahexa-1,5-diene-3,4-di-R-aminato, RN=C(H)(H)C(NR)(H)C(NR)C(H)=NR, the reductively C–C coupled formally dianionic dimer of R-DAB ligated to two metal atoms. 1,4,3a,6a-Tetrahydropyrrolo[3,2-*b*]pyrrole (Hantzsch-Widman nomenclature) is abbreviated as THPP. AIB stands for 3-amino-4-imino-1-butene, *t*-BuN=C(H)(N-*t*-Bu)C(CF_3)=CCF_3, the C–C coupling product between *t*-Bu-DAB and hexafluoro-2-butyne, ligated to two metal atoms. AIP stands for 1,2-diamino-2,3-diiminopropane, *t*-BuN=C(H)C(H)(N-*t*-Bu)C(N-*p*-Tol)=N-*p*-Tol, the C–C coupling product between *t*-Bu-DAB and *p*-Tol-carbodiimide, ligated to two metal atoms.

(2) Part I: Frühauf, H.-W.; Seils, F.; Romão, M. J.; Goddard, R. J. *Angew. Chem.* **1983**, *95*, 1014.

(3) Part II: Frühauf, H.-W.; Seils, F.; Goddard, R. J.; Romão, M. J. *Organometallics* **1985**, *4*, 948.

0276-7333/92/2311-3607$03.00/0

Scheme I

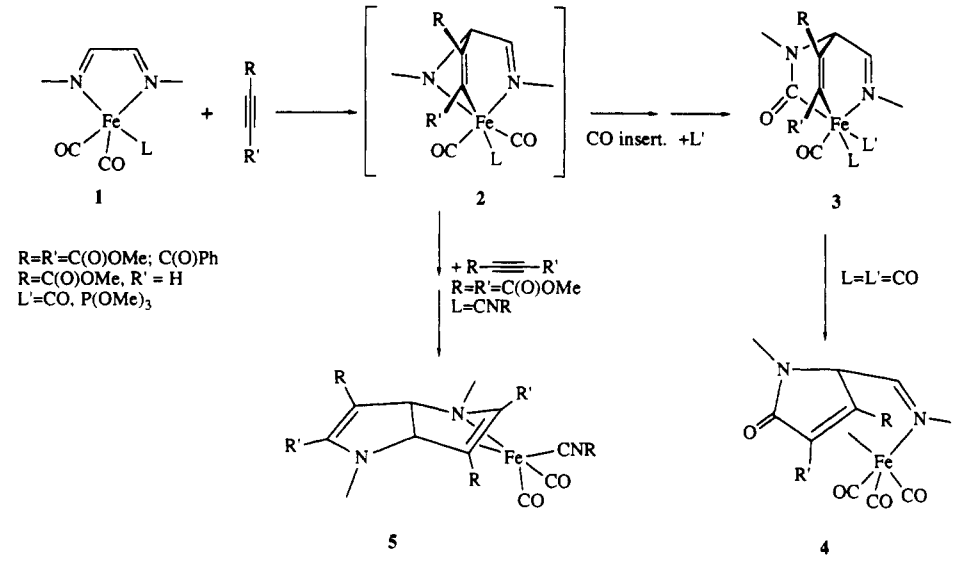

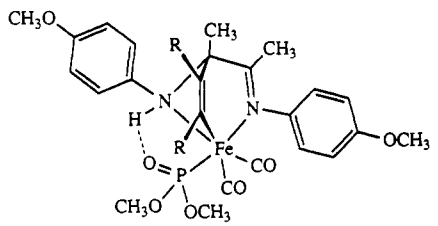

Figure 1. Molecular structure of the bicyclo[2.2.1] product resembling the initial cycloadduct 2.

adduct 2. Further evidence for the proposed mechanism, i.e., for the existence of the initial bicyclo[2.2.1] adduct with a definite lifetime, came from the reaction of Fe(CO)$_2$(CNR)(*i*-Pr-DAB) with dimethyl acetylenedicarboxylate (DMADC).[7] In this case, the reaction coordinate was found to branch at the stage of the initial cycloadduct giving either, intramolecularly, the CO-insertion product 3 or, intermolecularly, subsequent cycloaddition of another DMADC which results in formation of Fe(CO)$_2$(CNR)(THPP)[1] (5).

The availability of a novel synthetic approach toward Ru(CO)$_3$(R-DAB) complexes[8] prompted us to investigate the reactivity of Ru(CO)$_3$(*i*-Pr-DAB) toward electron-deficient alkynes. The objective was to see whether Ru(CO)$_3$(*i*-Pr-DAB) also demonstrates 1,3-dipolar reactivity toward activated alkynes and to compare its reactivity to that of the analogous iron complexes in order to extend our understanding of the factors influencing the C–C coupling reactions of coordinated R-DAB ligands. Furthermore we hoped that differences in the energetic barriers along the reaction coordinate, on changing from iron to ruthenium as the central metal atom, would allow us to detect or isolate hitherto unobserved intermediates.

In this paper we present the molecular structures of the bicyclo[2.2.2] complexes that are formed in the reaction of Ru(CO)$_3$(*i*-Pr-DAB) with DMADC in the presence of either CO or PPh_3 as additional ligand. The X-ray crystal structure of the latter will be described. By addition of HBF_4 at low temperature immediately after the cycloaddition, CO insertion was prevented which allowed us for the first time to isolate and characterize the initial bicyclo[2.2.1] complex. The X-ray molecular structure of this complex has been determined. The overall reaction mechanism and the mechanistic details will be discussed and compared with those of the analogous iron complexes.

Experimental Section

Materials and Apparatus. ^{1}H and ^{13}C NMR spectra were obtained on Bruker AC 100, WM 250, and AMX 300 spectrometers. IR spectra were recorded with a Perkin-Elmer 283 spectrophotometer, using matched NaCl cells. The variable-temperature IR measurements were performed on a Nicolet 7199B FT-IR spectrophotometer with a liquid nitrogen cooled HgCdTe detector. Elemental analyses were carried out by the section Elemental Analyses of the Institute for Applied Chemistry, TNO, Zeist, The Netherlands.

The solvents were carefully dried and distilled under nitrogen prior to use. All preparations were carried out under an atmosphere of dry nitrogen by conventional Schlenk techniques. $Ru_3(CO)_{12}$ and dimethyl acetylenedicarboxylate (DMADC) were used as purchased from Strem Chemicals, Inc., and Aldrich, respectively. $Ru_2(CO)_5$(*i*-Pr-ADA) was prepared from $Ru_3(CO)_{12}$ and *i*-Pr-DAB by published procedures.[9] For the preparation of Ru(CO)$_3$(*i*-Pr-DAB) the following procedure was used.[8] A suspension of 0.38 g (0.6 mmol) of $Ru_2(CO)_5$(*i*-Pr-ADA) in 120 mL of toluene was stirred under an atmosphere of CO (1.1 bar) for 15 min at 95 °C. During the reaction the color of the solution turned from orange to intense red and IR spectroscopy revealed an almost quantitative conversion of the starting compound to Ru(CO)$_3$(*i*-Pr-DAB) (>95%). Since on removal of the solvent under reduced pressure CO is split off and $Ru_2(CO)_5$(*i*-Pr-ADA) reformed, the reactions of Ru(CO)$_3$(*i*-Pr-DAB) with DMADC were carried out without isolation of the mononuclear complex.

Synthesis of Complex 9a. A freshly prepared solution of 1.2 mmol of Ru(CO)$_3$(*i*-Pr-DAB) in 120 mL of toluene (vide supra) was cooled to −78 °C, and a solution of 148 μL (1.2 mmol) of DMADC in 10 mL of toluene was added dropwise. The reaction mixture was warmed up to room temperature under an atmosphere of CO (1.1 bar) and stirred for an additional 12 h. The solvent was evaporated to dryness, and the residue was redissolved

(4) Part III: Frühauf, H.-W.; Seils, F. *J. Organomet. Chem.* **1986**, *302*, 59.
(5) Part IV: Frühauf, H.-W.; Seils, F. *J. Organomet. Chem.* **1987**, *323*, 67.
(6) Part V: Frühauf, H.-W.; Seils, F.; Stam, C. H. *Organometallics* **1989**, *8*, 2338.
(7) Part VI: de Lange, P. P. M.; Frühauf, H.-W.; van Wijnkoop, M.; Vrieze, K.; Wang, Y.; Heijdenrijk, D.; Stam, C. H. *Organometallics* **1990**, *9*, 1691.
(8) Mul, W. P.; Elsevier, C. J.; Frühauf, H.-W.; Vrieze, K.; Pein, I.; Zoutberg, M. C.; Stam, C. H. *Inorg. Chem.* **1990**, *29*, 2336.
(9) (a) Staal, L. H.; Polm, L. H.; Vrieze, K.; Ploeger, F.; Stam, C. H. *Inorg. Chem.* **1981**, *20*, 3590. (b) Staal, L. H.; Polm, L. H.; Balk, R. W.; van Koten, G.; Vrieze, K.; Brouwers, A. M. F. *Inorg. Chem.* **1980**, *19*, 3343.
(10) Schenk, H.; Kiers, C. T. *Simpel 83, a program system for direct methods*; Sheldrick, G. M., Kruger, C., Goddard, R., Eds.; Crystallographic Computing 3; Clarendon Press: Oxford, U.K., 1985.

in ca. 40 mL of diethyl ether. On cooling to −30 °C, the yellowish-white product precipitated overnight, and after concentrating the solvent to half its volume and subsequent cooling at −30 °C, a second batch of **9a** precipitated. Total isolated yield of **9a**: 0.42 g (70%).

Synthesis of Complex 9b. A freshly prepared solution of 1.2 mmol of $Ru(CO)_3$(*i*-Pr-DAB) in 120 mL of toluene (vide supra) was cooled to −78 °C, degassed, and a solution of 148 μL (1.2 mmol) of DMADC in 10 mL of toluene was slowly added. After the color of the solution had changed from deep red to yellow, 0.32 g of PPh_3 (1.2 mmol) was added and the reaction mixture was warmed up to room temperature. After removal of the solvent under reduced pressure the crude yellow-white product was washed three times with ca. 20 mL of cold diethyl ether and dried in vacuo (0.68 g, 80%). Crystals suitable for X-ray diffraction were obtained by diffusion of pentane into a solution of **9b** in THF at +4 °C for several weeks.

Synthesis of Complex 10. A freshly prepared solution of 1.2 mmol of $Ru(CO)_3$(*i*-Pr-DAB) in 120 mL of toluene (vide supra) was cooled to −78 °C, and a solution of 148 μL (1.2 mmol) of DMADC in 10 mL of toluene was added. After the color of the solution had changed from deep red to yellow, 0.3 mL of a solution of HBF_4 in diethyl ether (54%) was added and the reaction mixture was warmed up to room temperature. The solvent was evaporated to dryness, and the residue was dissolved in 5 mL of CH_2Cl_2. After addition of 40 mL of diethyl ether the white product precipitated which was washed three times with ca. 20 mL of diethyl ether and dried in vacuo (0.48 g, 70–75%). It was crystallized as off-white needles from a mixture of methanol and diethyl ether (2:1) at +4 °C or from tetrahydrofuran at −30 °C.

Synthesis of $Ru(CO)_3$(THPP)[1] (11). A suspension of 0.27 g (0.43 mmol) of $Ru_2(CO)_5$(*i*-Pr-ADA) in 120 mL of heptane was stirred under an atmosphere of CO (1.1 bar) for 15 min at 95 °C during which the color of the reaction mixture changed from pale orange to intense red. The starting complex was almost quantitatively converted to $Ru(CO)_3$(*i*-Pr-DAB) (>95%). After the solution of $Ru(CO)_3$(*i*-Pr-DAB) was cooled to −30 °C it was inversely filtered under positive N_2 pressure into a dropping funnel and then added dropwise during ca. 30 min to a solution of 230 μL (1.9 mmol) of DMADC in 50 mL of pentane at 0 °C. After the solution had been concentrated to ca. 30% of its volume at 0 °C, the solution was cooled to −80 °C upon which the yellowish-white product precipitated. After removal of the supernatant, the product was dried in vacuo (0.41 g, 80%). A satisfactory elemental analysis of complex **11** could not be obtained because the samples already showed some decomposition upon storage at ambient temperatures and were persistently contaminated with traces of impurities.

Crystal Structure Determination of 9b and 10. The crystallographic data for the complexes **9b** and **10** are listed in Table I. The reflections were measured on a Nonius CAD4 diffractometer (25 °C, θ–2θ scan) using graphite-monochromated Cu Kα radiation. Reflections with an intensity below the $2.5\sigma(I)$ level were treated as unobserved.

The non-hydrogen atoms in **9b** were found by using the method of Patterson-minimum-function and the hydrogen atoms were found in a ΔF synthesis. The refinement of the non-hydrogen atoms proceeded using isotropic block-diagonal least-squares calculations. An empirical absorption correction (DIFABS)[11] was applied.

The position of the Ru atom in **10** was determined by direct methods using the program Simpel83.[10] The remaining non-hydrogen atoms were found in a ΔF synthesis. The positions of the hydrogen atoms of **10** were calculated and refined using isotropic block-diagonal least-squares calculations. The refinement of the non-hydrogen atoms proceeded using anisotropic block-diagonal least-squares calculations. An empirical absorption correction (DIFABS)[11] was applied.

The calculations were performed with XRAY76,[12] the atomic scattering factors were taken from Cromer and Mann,[13] and the dispersion corrections were taken from ref 14.

Table I. Crystallographic Data and Details of Data Collection and Refinement for 9b and 10

	9b	**10**
(a) Crystal Parameters		
formula	$C_{35}H_{37}N_2O_7PRu \cdot 0.5C_4H_8O$	$C_{17}H_{23}N_2O_7Ru^+BF_4^-$
fw	765.7	555.3
cryst syst	orthorhombic	orthorhombic
space group	*Pnca*	*Pbca*
a, Å	18.699 (1)	13.5335 (8)
b, Å	34.331 (2)	17.088 (1)
c, Å	11.530 (1)	20.645 (2)
V, Å^3	7401.7	4774.4 (6)
$d_{(calc)}$, g/cm^3	1.37	1.55
Z	8	8
approx cryst size, mm^3	0.10 × 0.25 × 0.38	0.20 × 0.43 × 0.88
(b) Data Collection		
radiation (λ, Å)	Cu Kα (1.5418)	Cu Kα (1.5418)
μ, cm^{-1}	43.2	60.7
monochromator	graphite	graphite
θ_{max}, deg	65	70
total no. of unique reflctns	6271	4523
obsd data ($I > 2.5\sigma(I)$)	5193	3634
h min, max	0, 21	0, 16
k min, max	0, 40	0, 20
l min, max	0, 13	0, 25
abs corr	DIFABS[11]	DIFABS[11]
X-ray exposure, h	74	50
(c) Refinement		
no. of params	590	382
weighting scheme	$1/(7.0 + F_o + 0.007F_o^2)$	$1/(7.92 + F_o + 0.006F_o^2)$
final *R* values	$R = 0.031$ ($R_w = 0.061$)	$R = 0.040$ ($R_w = 0.061$)
res density (min, max), e Å^{-3}	−0.3, 0.5	−0.3, 0.8
anomalous scattering	Ru	Ru
max shift/error	0.6758	0.89

Results and Discussion

An in situ prepared solution of $Ru(CO)_3$(*i*-Pr-DAB) in toluene reacted instantly at −78 °C with 1 equiv of DMADC. Depending on the kind of additional ligand offered to the solution, different products were obtained (Scheme II).

When the reaction mixture was allowed to warm to room temperature under an atmosphere of CO (1.1 bar) and stirred for an additional 12 h under the same conditions, the bicyclo[2.2.2] complex **9a** could be isolated in good yield. The structure of **9a** has been tentatively assigned on the basis of its IR and NMR (^{1}H, ^{13}C) spectroscopic properties. In contrast with the analogous iron complex[3] which thermally isomerizes to form a (1,5-dihydropyrrol-2-one)$Fe(CO)_3$ complex (**4**), complex **9a** is thermally stable and does not, even at temperatures up to 50 °C, show any conversion to the rearrangement product. Though Ru–C bonds are generally considered to be stronger than Fe–C bonds, it is evident from the crystal structure of **9b** (vide infra) that the two Ru–C bonds in question are comparatively long. Since the destabilizing trans influence of the additional CO ligand in **9a** would tend to elongate at least one of these Ru–C bonds even further, the observed thermal stability cannot be easily accounted for. The reactivity the analogous Fe complexes[2,3] clearly demonstrates that this reductive elimination is sensitive to small changes in the electronic and steric properties of both the

(11) Walker, N.; Stuart, D. *Acta Crystallogr.* **1983**, *A39*, 158.
(12) Stewart, J. M. The XRAY76 system. Technical Report TR446; Computer Science Center, University of Maryland: College Park, MD, 1976.
(13) Cromer, D. T.; Mann, J. B. *Acta Crystallogr.* **1968**, *A24*, 321.
(14) *International tables for X-Ray Crystallography*; Kynoch Press: Birmingham, U.K., 1974; Vol. IV.

Scheme II

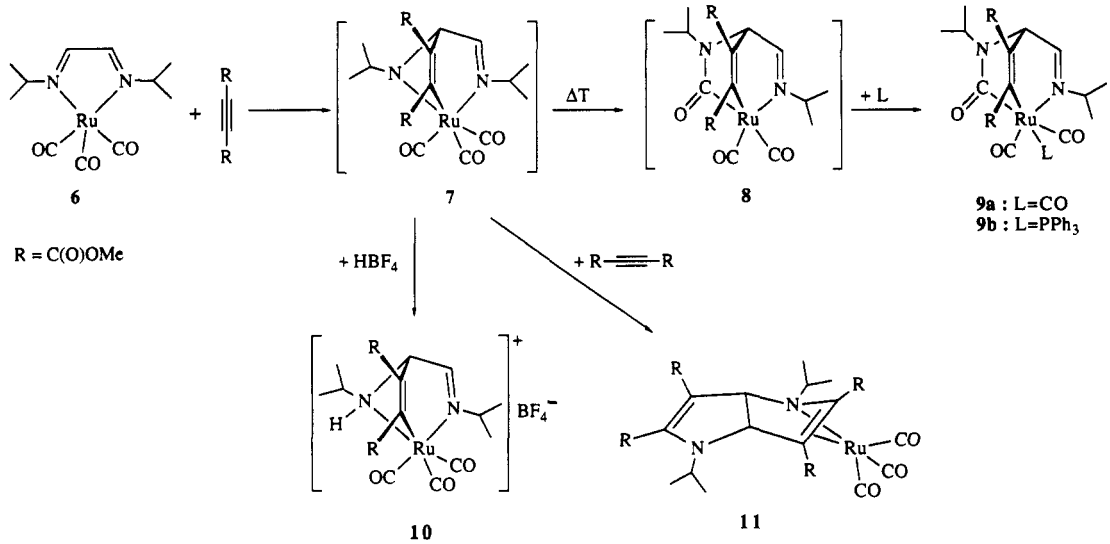

ligand system and the metal. So perhaps in complex **9a** the observed decrease in carbanionic character (from the ^{13}C NMR) of the carbon atoms, that are available for the reductive elimination, has a two-way effect; on one hand it tends to elongate the Ru–C bonds but on the other hand it disfavors the attack of the former alkyne C atom on the inserted carbonyl.

When PPh_3 was added after the cycloaddition and the reaction mixture was allowed to warm to room temperature the white bicyclo[2.2.2] complex **9b** was formed. Complex **9b** has been characterized both spectroscopically and by X-ray crystallography. As in the analogous Fe complexes,[3] the additional ligand in complex **9b** occupies a position trans to the carbon atom of the inserted carbonyl group, which brings about an unusually large $^2J_{P\text{-}M\text{-}C}$ (>80 Hz) on the ^{13}C resonance of this carbon atom. On account of the increased radius of ruthenium (as compared with iron), the large PPh_3 ligand can be coordinated to the ruthenium center without distortion of the octahedral coordination geometry, whereas in the case of the analogous iron complexes only phosphites with small cone angles (such as $P(OCH_3)_3$) could be used to stabilize the bicyclo[2.2.2] structure.

Addition of HBF_4 at low temperature (−78 °C) to the reaction mixture immediately after the cycloaddition results in the formation of the cationic bicyclo[2.2.1] complex **10**. Its molecular structure was established by an X-ray crystal structure determination, which will be discussed below. By protonation of the former imine N atom, the nucleophilic attack of this N atom on one of the terminal CO ligands is prevented and the molecular geometry of the bicyclo[2.2.1] intermediate **7** is retained. The formation of the cationic complex **10** strongly supports the 1,3-dipolar cycloaddition mechanism proposed for the initial step in this type of reaction.

Reaction of $Ru(CO)_3$(*i*-Pr-DAB) with an excess of DMADC results in the formation of $Ru(CO)_3$THPP (**11**) in high yield. This type of reactivity was also observed for activated $Fe(CO)_2$CNR(R-DAB) complexes and has been described, together with the mechanistic details, in part 6 of this series.[7] The formation of the heterocyclic THPP ligand is the result of subsequent 1,3-dipolar cycloadditions of two molecules of DMADC to both C=N—Ru units followed by two reductive eliminations. The fact that THPP formation is also observed for the $Ru(CO)_3$(*i*-Pr-DAB) complex furthermore suggests an increase in reactivity of this complex in comparison to $Fe(CO)_3$(*i*-Pr-DAB) because for the latter complex, substitution of a terminal carbonyl for a σ-donating CNR ligand is a prerequisite for the second cycloaddition. A possible explanation for the increased reactivity of the Ru complex based on electronic and steric arguments will be given in the section on complex formation. In contrast to the $Fe(CO)_2$(CNR)THPP complex, $Ru(CO)_3$THPP is not thermally stable and the newly formed heterocyclic ligand readily dissociates from the metal[15] at slightly elevated temperatures ($T > 30$ °C), whereas the Fe complex has to be oxidatively degraded. The thermal lability of complex **11** prompted us to search for a catalytic way to synthesize these highly functionalized THPP heterocycles. However, attempts to directly displace the heterocycle from the metal by *i*-Pr-DAB at slightly elevated temperatures did not result in reformation of the starting complex $Ru(CO)_3$(*i*-Pr-DAB). Other possibilities to regenerate the starting compound in order to close the catalytic cycle are currently being investigated.

Complex Formation. Due to the increased stability of the intermediates in the reaction sequence of $Ru(CO)_3$(*i*-Pr-DAB) it was possible to obtain more detailed information on the mechanistic aspects of the described reaction. It is now firmly established (both by the formation of the bicyclo[2.2.1] complex **10** and $Ru(CO)_3$THPP **11** as well as by LT-FTIR spectroscopy) that the first step in these reactions is a 1,3-dipolar cycloaddition of the alkyne over the Ru—N=C fragment giving the bicyclo[2.2.1] intermediate **7**. The fact that this first step instantly proceeds at −78 °C indicates that the activation energy for the initial 1,3-dipolar cycloaddition is lower than for the corresponding iron complexes. In order to explain the increased reactivity of the Ru complex, both organometallic 1,3-dipoles M—N=C can be compared with the isolobally related organic azomethine ylide.[6] According to the Sustmann classification[16] the azomethine ylide is a type

(15) The thermal decomposition of $Ru(CO)_3$THPP (**11**) results in liberation of the intact C_2-symmetric *i*-Pr-THPP ligand of which the ^1H and ^{13}C NMR data have been reported by us in a previous publication; see refs 7 and 31. The $Ru(CO)_3$ fragments recombine to give a small amount of $Ru_3(CO)_{12}$ and some metallic deposit.

(16) Application of the frontier molecular orbital theory to 1,3-dipolar cycloadditions by Sustmann provides a semiquantitative classification of these cycloadditions into three types depending on the relative disposition of the 1,3-dipole and the dipolarophile frontier orbitals. (a) Sustmann, R. *Tetrahedron Lett.* **1971**, 2717. (b) Sustmann, R.; Trill, H. *Angew. Chem., Int. Ed. Engl.* **1972**, *11*, 838. (c) Sustmann, R. *Pure Appl. Chem.* **1974**, *40*, 569.

I or nucleophilic dipole, which implies that it possesses a relatively high-lying HOMO and LUMO and reacts preferentially with electron-deficient dipolarophiles. Cycloaddition reactions of a nucleophilic 1,3-dipole are HOMO-controlled (i.e., the interaction of the dipole HOMO with the dipolarphile LUMO is predominant). On the basis of the previous remarks, HOMO control is proposed for the organometallic dipoles. This is supported by theoretical CAS–SCF calculations performed by Dedieu et al. on both the model systems $M(CO)_3(HN{=}C(H){-}C(H){=}NH)$ (M = Fe, Ru) and the parent azomethine ylide.[17] They indicate that the HOMO levels of the organometallic 1,3-dipoles are found at slightly higher energy than the one of the organic ylide and that the organometallic dipoles possess more diradical character.[18] Application of perturbation theory to 1,3-dipolar cycloaddition reactions[19] shows that for the HOMO-controlled reaction both a decrease in the HOMO–LUMO gap, which is associated with an increase in diradical character, as well as a higher HOMO energy, will accelerate the reaction. Comparison of $Ru(CO)_3$(*i*-Pr-DAB) with the analogous iron complex, based on the CAS-SCF calculations, shows that both complexes possess roughly the same amount of diradical character. We therefore assume that the HOMO level of the ruthenium complex is slightly higher in energy (i.e., the dipole is more nucleophilic). This is supported by the observation that in the case of ruthenium there is less π-back-donation to the terminal carbonyl ligands (IR and ^{13}C NMR) which implies a higher electron-density on the central metal atom. We note that steric influences can also play an considerable role; the approach of the activated alkyne is probably facilitated on the ruthenium complex.

The subsequent reaction of the bicyclo[2.2.1] intermediate **7** depends on the nature of the ligand offered. Addition of HBF_4 stabilizes the bicyclo[2.2.1] structure and gives rise to the formation of complex **10**. In the presence of excess alkyne intermediate **7** undergoes a second cycloaddition which finally results in formation of complex **11**. An explanation for this increased reactivity in comparison to $Fe(CO)_3$(*i*-Pr-DAB) is based on the same arguments used for the first cycloaddition. The substitution of iron for ruthenium has more or less the same effect as the substitution of a terminal carbonyl ligand for a σ-donating CNR in $Fe(CO)_3$(*i*-Pr-DAB); in both cases the electron-density on the central metal atom increases which enables the second cycloaddition to the remaining M—N=C dipole. Again, the decline of steric constraint may also contribute to the increased reactivity. If there is no reaction partner for an intermolecular reaction of **7** (protonation or second cycloaddition), a nucleophilic attack of the former imine N atom on a terminal CO ligand in complex **7** occurs at ca. −40 °C which results in the formation of the 16-electron complex **8**. Although this species appears to be coordinatively unsaturated, it is relatively stable in the absence of an additional ligand. This is probably the result of an inter- or intramolecular O coordination by an ester carbonyl moiety of the alkyne to the electrophilic Ru^{2+} center. Several examples of this type of coordination have been reported in the literature.[20] The spectroscopic data for complex **8** provide support for this proposal.[21] In the IR spectrum one of the absorptions assigned to the organic C=O fragments is observed at a relatively low frequency (1605 cm^{-1}), which is indicative of a C=O—Ru interaction.[20a,d] In addition the ^{13}C spectrum shows a resonance at a rather high δ value (222.0 ppm), which, in agreement with the values reported by Guilbert et al.,[20c] is assigned to the coordinated ester carbonyl carbon atom. An intramolecular interaction, comparable to the one reported by Torres et al.,[20a] will in the case of **8** lead to the formation of an additional four-membered heterometallacycle (see Figure 2). Alternatively complex **8** can be stabilized by an intermolecular interaction, with one of the ester carbonyl O atoms on one Ru atom coordinated to a second Ru unit and vice versa, resulting in an eight-membered heterodimetallacycle. This type of coordination has been described by Lindner et al. in reactions of $Ru(CO)_4(\eta^2$-ethene) with activated alkynes.[20b] We have not been able to exclude one of the possibilities on the basis of the present data. In view of the distortion that the formation of an additional four-membered ring would impose, we tend to favor the dinuclear interaction. However, this would require a highly symmetric dimer, since only one set of resonances is observed in the ^{13}C NMR. In the presence of CO or PPh_3

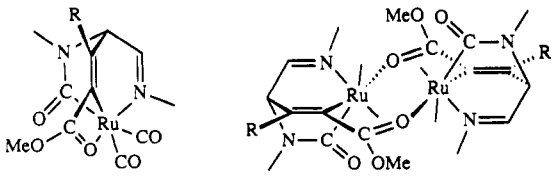

Figure 2. Intra- and intermolecular stabilization of complex **8**.

Table II. IR Frequencies and Elemental Analyses

		elemental analyses		
compd	IR ν(CO), cm^{-1}	C obs (calc)	H obs (calc)	N obs (calc)
9a	2102 (s), 2039 (s)	not analyzed		
9b	2040 (s), 1984 (s)	57.94 (58.03)	5.27 (5.40)	3.40 (3.66)
10	2130 (s), 2078 (s), 2051 (s)	36.68 (36.77)	3.94 (4.18)	5.03 (5.05)
11	2069 (s), 1997 (s), 1989 (sh)	not analyzed		

(17) The CAS-SCF (complete active space self-consistent field) method is a particular case of the MCF-SCF (multiconfiguration self-consistent field) method. In the MS-SCF method the wave function Ψ is expanded over electron configurations Φ, $\Psi = \sum C_i\Phi_i$, and in the variation process both the coefficients C_i of the expansion and the electronic configurations Φ_i (or more precisely the orbitals on which the Φ_i's are built) are optimized (see: Salahub, D. R.; Zerner, M. C. *The challenge of d- and f-electrons*; ACS Symposium Series 394; American Chemical Society: Washington, DC, 1989). The CAS-SCF calculations were performed by M. J. Liddell and A. Dedieu, Université Louis Pasteur, Strasbourg, and will be published in a forthcoming paper.

(18) Theoretical studies indicate that 1,3-dipoles can, apart from the zwitterionic VB structures, also be described in terms of a spin-paired 1,3-diradical structure. The larger the contribution of the diradical structure to the wave function, the more diradical character a 1,3-dipole possesses. In terms of MOs the diradical character can be seen as a depopulation of the HOMO to the benefit of the LUMO. A decrease in the HOMO–LUMO gap leads to increasing degeneracy of the HOMO and the LUMO (more configuration interaction) and therefore an increase in diradical character. Houk, K. N.; Yamaguchi, K. In *1,3-Dipolar Cycloaddition Chemistry*; Padwa, A., Ed.; John Wiley and Sons Inc.: New York, 1984; Chapter 13.

(19) (a) Houk, K. N.; Sims, J.; Duke, R. E., Jr.; Strozier, R. W.; George, J. K. *J. Amer. Chem. Soc.* **1973**, *95*, 7287. (b) Houk, K. N.; Sims, J.; Watts, C. R.; Luskus, L. J. *J. Amer. Chem. Soc.* **1973**, *95*, 7301.

(20) (a) Torres, R. M.; Santos, A.; Ros, J.; Solans, X. *Organometallics* **1987**, *6*, 1091. (b) Lindner, E.; Jansen, R.-M.; Mayer, H. A.; Hiller, W.; Fawzi, R. *Organometallics* **1989**, *8*, 2355. (c) Guilbert, B.; Demerseman, B.; Dixneuf, P. H.; Mealli, C. *J. Chem. Soc., Chem. Commun.* **1989**, 1035. (d) Blackmore, T.; Bruce, M. I.; Stone, F. G. A. *J. Chem. Soc., Dalton Trans.* **1974**, 106.

(21) The spectroscopic data of complex **8** at 243 K. IR ν(CO): 2041 (s), 1977 (s), 1710 (m), 1685 (m), 1605 (m) cm^{-1}. ^1H NMR (300.13 MHz), δ: 8.26 (1 H, d, 5 Hz, N=CH); 5.81 (1 H, d, 5 Hz, N—CH); 4.75, 4.30 (2 × 1 H, 2 × sept, 6.5 Hz, *i*-Pr—CH); 3.79, 3.68 (2 × 3 H, 2 × s, OCH_3); 1.25, 1.14, 1.12, 0.92 (4 × 3 H, 4 × d, 6.5 Hz, *i*-Pr—CH_3). ^{13}C NMR (75.47 MHz), δ: 222.0 (C=O—Ru); 201.0, 194.7, 192.6 (2 × CO, Ru—C=C); 179.7 (Ru—C=O); 166.8 (C=N); 161.2 ($C(O)OCH_3$); 124.5 (Ru—C=C); 58.8 (*i*-Pr-C); 55.9 (C—N); 53.0, 52.2 ($C(O)OCH_3$); 42.9 (*i*-Pr—C); 24.4, 23.4, 22.9, 21.2 (*i*-Pr—CH_3).

Table III. ^{1}H NMR Data for Complexes 9a, 9b, and 10

	δ, mult, coupl const, rel intens		
compd	9a[a]	9b[a]	10[b]
nucleus			
H(6)	3.80, s, 3 H	2.87, s, 3 H	3.89, s, 3 H
H(7)	3.91, sept, 6.6, 1 H	3.55, sept, 6.4, 1 H	4.15, sept, 6.4, 1 H
H(8), H(9)	1.05, d, 6.8, 6 H	1.02, d, 6.7, 6 H	1.46, d, 6.4, 3 H
			1.30, d, 6.4, 3 H
H(12)	3.73, s, 3 H	3.66, s, 3 H)	3.79, s, 3 H
H(13)	5.75, d, 5.3, 1 H	5.72, d, 5.4, 1 H	5.68, dd, 2.7, 0.8, 1 H
H(14)	8.43, d, 5.3, 1 H	8.33, d, 5.4, 1 H	8.46, d, 2.7, 1 H
H(15)	4.84, sept, 6.8, 1 H	4.88, sept, 6.7, 1 H	3.17, d sept, 9.9, 6.4, 1 H
H(16), H(17)	1.30, d, 6.6, 3 H	1.17, d, 6.4, 3 H	1.33, d, 6.3, 3 H
	1.28, d, 6.6, 3 H	0.50, d, 6.4, 3 H	1.32, d, 6.3, 3 H
H(19)–H(22)		7.34, m, 15 H	
N–H			5.64, d (br), 9.9, 1 H

[a] δ values (in ppm, relative to TMS) have been measured in $CDCl_3$ solution at 293 K and 100.1 MHz. [b] Measured at 300.13 MHz. [c] s = singlet, d = doublet, dd = double doublet, sept = septet, m = multiplet, and br = broad. Coupling constants are given in hertz.

complex 8 reacted to give the stable bicyclo[2.2.2] complexes **9a** and **9b**, respectively. The reaction with PPh_3 is somewhat faster probably because this σ-donor is more effective in substituting the coordinated O atom.

IR Spectroscopy: ν(CO) and ν(N–H) Regions. The ν(CO) absorption patterns and band positions of the bicyclic products **9a**, **9b**, and **10**, listed in Table II, show characteristic differences reflecting the changes in the amount of π-back-donation to the terminal CO ligands associated with the electron density on the central ruthenium atom.

In compound **10** the CO stretching vibrations give rise to three separate absorptions at unusually high frequencies, indicating that there is very little π-back-donation due to the formal oxidation state Ru(II) and the cationic nature of the complex. The CO ligands of **9a** give rise to one sharp and one broad absorption band at relatively high frequency which is again attributed to the electron-poor ruthenium center (the positions can be compared with those in $Ru(CO)_3X(CH_3C{=}C(H)C(H){=}N\text{-}i\text{-}Pr)$ (X = Cl, Br, I)).[22] On account of the σ-donor ligand PPh_3, which enhances the electron-density on the metal, the two slightly broadened CO absorptions of **9b** are found at low frequencies compared with **9a** and **10**. The absorption patterns of **9a** and **9b** are similar to those of the analogous iron complexes,[2,3] but the absorptions are shifted to higher frequencies reflecting the commonly observed decrease in π-back-donation of ruthenium compared with iron.[8,23] In all three bicyclic complexes the ester C=O's appear as one broad absorption between 1690 and 1715 cm^{-1}. In order to elucidate the reaction mechanism, the reaction was monitored by LT-FTIR spectroscopy. The earliest observable intermediate shows three CO absorptions at high frequencies (2123 (s), 2067 (s), 2008 (s) cm^{-1}) which are comparable to those of compound **10** and are therefore assigned to the initial [2.2.1] cycloadduct **7**. Upon a raise in temperature, **7** converts into compound **8** which shows two terminal CO absorptions of equal intensity at comparatively low frequencies (2041 (s), 1977 (s) cm^{-1}). In Scheme II compound **8** is depicted as a coordinatively unsaturated 16-electron complex, but it is probably stabilized either by inter or intramolecular interactions (vide supra). After addition of CO or PPh_3 to the reaction mixture, **8** is converted to **9a** or **9b**, respectively.

The new N–H bond in **10** gives rise to an absorption in the ν(N–H) region at 3205 cm^{-1}, which is significantly lower

Table IV. ^{13}C NMR Data for Complexes 9a, 9b, and 10 (Atomic Numbering as in Figure 3)

	δ, ppm[a]		
compd	9a	9b (^nJ(C,P))[b]	10
nucleus			
C(1–3)	198.0	199.6 (6.8)	190.6
	192.3	197.9 (6.8)	189.7
	189.7		188.3
C(4)	188.5	192.0 (7.5)	184.6
C(5)	177.5	177.2 (3.8)	174.7
C(6)	52.3	52.8	53.7
C(7)	66.3	64.5 (4.5)	65.2
C(8,9)	23.2	21.4	24.3
	22.9	21.4	24.2
C(10)	125.5	127.7 (4.0)	130.2
C(11)	161.0	163.6	160.8
C(12)	51.3	50.8	53.2
C(13)	54.6	55.9	68.8
C(14)	170.1	168.6	173.8
C(15)	41.7	42.9	54.2
C(16,17)	21.6	25.8	23.6
	20.1	23.0	20.9
C(18)	184.8	199.5 (83.0)	
C(19)		134.0 (34.5)	
C(20)		129.1 (9.8)	
C(21)		134.3 (11.3)	
C(22)		130.8	

[a] δ values (in ppm, relative to TMS) have been measured in $CDCl_3$ solution at 243 K and 74.47 MHz. [b] Coupling constants in hertz.

Table V. ^{1}H NMR and ^{13}C NMR Data for Complex 11 (Numbering as in Figure 3)

	^{1}H NMR δ, mult, coupl const[b,c]	^{13}C NMR δ[a]
nucleus		
1–3		200.3
		199.3
		197.0
4[d]		86.7
5[d]		170.0
6[d]	3.44, s, 3 H	51.8
7[d]		95.8
8[d]		164.1
9[d]	3.40, s, 3 H	53.1
10	3.90, sept, 6.9, 1 H	58.1
11, 12	1.04, d, 7.0, 3 H	19.1
	1.20, d, 7.0, 3 H	20.4
13	4.86, d, 8.9, 1 H	73.1
14	4.45, d, 8.9, 1 H	72.0
15[d]		56.0
16[d]		197.4
17[d]	3.35, s, 3 H	50.9
18[d]		79.0
19[d]		173.9
20[d]	3.33, s, 3 H	52.9
21	3.83, sept, 6.8, 1 H	68.9
22, 23	1.23, d, 6.8, 1 H	21.0
	1.36, d, 6.7, 1 H	24.6

[a] δ values (in ppm, relative to TMS) have been measured in C_6D_6 solution at 283 K and 75.47 MHz. [b] δ values (in ppm, relative to TMS) have been measured in C_6D_6 solution at 283 K and 300.13 MHz. Coupling constants in hertz. [c] s = singlet, d = doublet, sept = septet, m = multiplet, and br = broad. [d] Individualized assignment for respective sets of signals are tentative.

(22) Mul, W. P.; Elsevier, C. J.; van Leijen, M.; Spaans, J. *Organometallics* **1991**, *10*, 251.
(23) van Dijk, H. K.; Stufkens, D. J.; Oskam, A. *J. Am. Chem. Soc.* **1989**, *111*, 541. See also ref 27c.

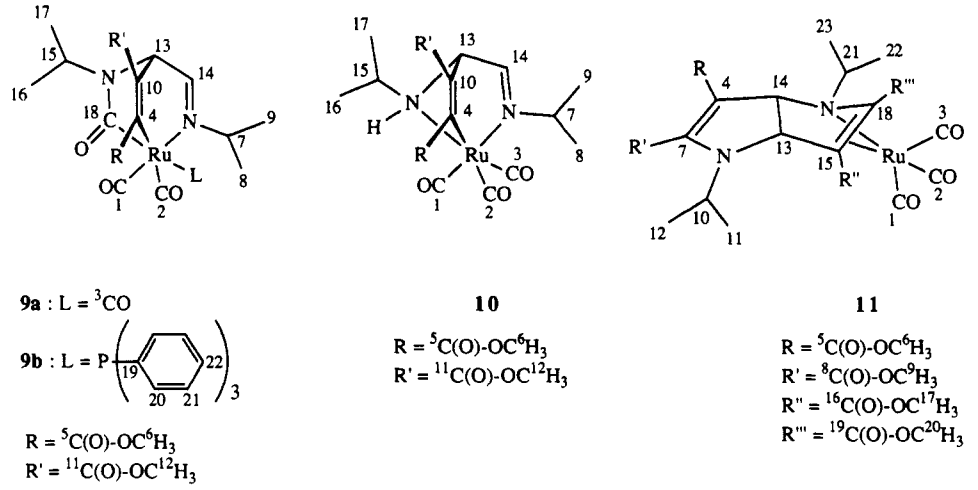

Figure 3. Atomic numbering scheme for the ^1H and ^{13}C NMR data of complexes **9–11**.

than those reported for $FeM(CO)_6[RNC(R^1)C(R^2)N(H)R]$ (M = Mn, Re)[24] and $Ru_2(CO)_6[R^1CC(H)C(H)N(H)R^2]$[25] observed between 3275 and 3305 cm^{-1}. This suggests a weaker N–H bond resulting in an increased acidity of the N–H proton. This is also evident from the position of the N–H proton resonance in the ^1H NMR (vide infra).

^1H and ^{13}C NMR Spectroscopy. The ^1H and ^{13}C NMR data of **9a**, **9b**, and **10** are listed in Tables III and IV, respectively; the atomic numbering is given in Figure 3. The ^1H and ^{13}C NMR data of complex **11**, listed in Table V (atomic numbering as in Figure 3), will be discussed separately. The NMR spectra of compounds **9b** and **10** in solution are in agreement with the molecular structure in the solid state.

In compounds **9a**, **9b**, and **10** the former imine protons H(13) are shifted ca. 2.5 ppm upfield in comparison to the intact imine protons H(14) that resonate at approximately 8.4 ppm. This reflects the change in hybridization from sp^2 to sp^3, due to the C–C coupling of the former imine carbon atom C(13). In both **9a** and **9b** the ^3J coupling between H(13) and H(14) is ca. 5.5 Hz which is in agreement with the analogous iron complexes,[3] in complex **10**, however, this coupling constant is significantly smaller (2.7 Hz), indicating a larger dihedral angle between the C–H bonds as a consequence of the distorted geometry of the bicyclic moiety of this complex. The N–H proton in **10** resonates at 5.64 ppm, which is ca. 3 ppm downfield compared with the N–H resonance in $Ru_2(CO)_6[R^1CC(H)C(H)N(H)R^2]$[25] and indicates an increase in acidity of this proton. The very large ^3J coupling between the N–H and the *i*-Pr–CH (H(15)) protons (^3J = 9.9 Hz) indicates that the N–H and *i*-Pr–C–H bonds are nearly coplanar whereas the dihedral angle between the N–H and C–H(13) bonds is probably close to 90°, which is reflected in a small ^3H coupling of 0.8 Hz (Karplus–Conroy relation). Since complex **10** contains two independent chiral centers, i.e., the former imine N atom and the bridgehead C atom,[26] it may exist in two diastereomeric configurations. However, both ^1H and ^{13}C NMR show only one set of resonances for the bicyclic moiety in **10**, pointing to the presence of only one diastereomer. In the bicyclic **9a** and **10**, the inequivalent carbomethoxy groups of the former DMADC appear as two singlets between 3.6 and 3.9 ppm. This difference is much larger for complex **9b** where one of the carbomethoxy resonances is shifted upfield by ca. 1 ppm, probably due to the proximity of one of the anisotropic phenyl groups of the additional ligand PPh_3 (this is confirmed by the structure in the solid state). The diastereotopic *i*-Pr–methyl groups give rise to either three (**9a** and **9b**) or four doublets (**10**) in the ^1H NMR spectrum, and the respective carbon atoms appear as three or four signals between 20 and 26 ppm in the ^{13}C NMR. The carbonyl carbon atoms of **9a** resonate between 189.7 and 198.0 ppm, which is ca. 7 ppm upfield compared with those in the corresponding Fe complex.[3] This can be attributed to a slight decrease in π-back-donation to the terminal CO ligands, a feature commonly observed on going from Fe to Ru.[27] The ^{13}C resonances of the CO ligands of **10** are found at even higher field (188.3–190.6 ppm), reflecting a further decrease in π-back-donation, consistent with the cationic nature of this complex. Compared to **9a**, the carbonyl carbon atoms of **9b** are shifted downfield (197.9 and 199.6 ppm) as a consequence of the substitution of a π-accepting CO ligand for the σ-donor PPh_3. The resonance of the intact imine carbon atom C(14) in all three complexes is shifted ca. 30 ppm downfield in comparison to $Ru(CO)_3$(*i*-Pr-DAB) which is probably the result of a decrease in π-back-donation of the Ru(II) center to this isolated imine fragment. The former alkyne carbon atom C(10) in complexes **9a**, **9b**, and **10** resonates at 125.5, 127.7, and 130.2 ppm, respectively, which is within the range normally observed for sp^2-hybridized carbon atoms. The additional lowfield shift of 55–60 ppm found for the metal-bonded, sp^2-hybridized C(4) in all three complexes is probably caused by the σ bond to the metal which enhances the carbanionic character of this carbon atom, resulting in unusual high paramagnetic shielding. Similar values for this type of carbon atom are observed in $RuLL'\{C(CO_2Me)=CH(CO_2Me)\}(\eta\text{-}C_5H_5)$ complexes.[28] From the $^2J_{C\text{-}M\text{-}P}$ coupling constants in **9b** it can be concluded that also in solution the additional ligand PPh_3 is positioned trans to the inserted carbonyl C(18). This is evident from the extremely large $^2J_{C\text{-}M\text{-}P}$ of 83 Hz found for this carbon atom (C(18)), which is even larger than in the analogous Fe complex (78.5 Hz) and exceeds values given in the literature[29] by ca. 40 Hz. Also, the relatively

(24) Keijsper, J.; Mul, W. P.; van Koten, G.; Vrieze, K.; Ubbels, H. C.; Stam, C. H. *Organometallics* **1984**, *3*, 1732.
(25) Mul, W. P.; Elsevier, C. J.; van Leijen, M.; Vrieze, K.; Smeets, W. J. J.; Spek, A. L. *Organometallics* **1992**, *11*, 1877.
(26) We note that the central ruthenium atom is chiral too. However its chirality is directly related to that of the bridgehead carbon atom.
(27) (a) Todd, L. J.; Wilkinson, J. R. *J. Organomet. Chem.* **1974**, *77*, 1. (b) Pregosin, P. S. *Annu. Rev. NMR Spectrosc.* **1981**, *11a*, 227 and references therein. (c) Muller, F. Ph.D. Thesis, University of Amsterdam, 1988.
(28) Bruce, M. I.; Catlow, A.; Humphrey, M. G.; Koutsantonis, G. A.; Snow, M. R.; Tiekink, E. R. T. *J. Organomet. Chem.* **1988**, *338*, 59.

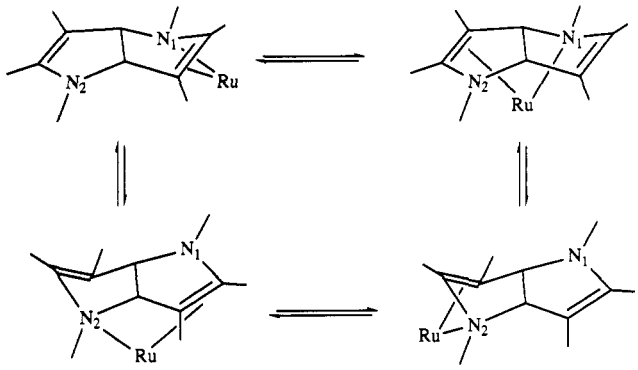

Figure 4. Proposed mechanism for the dynamic behavior of complex 11.

small $^2J_{C-M-P}$ values for the remaining Ru-bonded C atoms (C(1), C(2), C(4)), ranging from 6.8 to 7.5 Hz, clearly indicate that they are positioned cis to PPh_3. Heteronuclear 2D-correlated NMR spectroscopy has been used to assign the resonances of the two methine carbon atoms (C(7) and C(15)) and of the bridgehead carbon atom (C(13)) in complexes **9b** and **10**. In compound **10** the bridgehead carbon atom C(13) resonates at 68.8 ppm, which is ca. 13 ppm further downfield than in **9a** and **9b** (54.6 and 55.9 ppm, respectively). In all three complexes the methine carbon atom C(7) is observed at ca. 65 ppm. The resonance of the proton attached to C(7) however shows a pronounced dependence on the amount of σ donation by the imine nitrogen atom, which in its turn depends on the electron density on the central ruthenium atom, and is shifted upfield in the order **9b < 9a < 10**.

One of the possible modes of coordination for the $Ru(CO)_3$(THPP) complex **11**, with one ring of the bicyclic ligand σ-N- and π-C=C-coordinated to the $Ru(CO)_3$ fragment, is depicted in Figure 3. This type of coordination has also been observed for the $Fe(CO)_2$(CN-*t*-Bu)-(THPP) complex in the solid state.[7] In solution however, both ^1H and ^{13}C NMR indicate a complex dynamic behavior, involving several coordination isomers of complex **11**.

At 283 K the ^1H NMR of **11** (in $CDCl_3$ and in C_6D_6) shows two separate sets of resonances of unequal intensity. The set of resonances of minor intensity (ca. 30%) consists of a singlet resonance for the former imine protons (H(13) and H(14)), one septet for the methine protons (H(10) and H(21)) and two singlets for the ester protons (H(6), H(9), H(17), H(20)) and is therefore assigned to a C_2-symmetric σ-N,σ-N′-coordinated THPP ligand.[30] From 283 K down to 213 K this coordination isomer is present in solution and shows no exchange with the other isomers. At slightly elevated temperatures (303–313 K) the resonances belonging to σ-N,σ-N′$Ru(CO)_3$(THPP) appear to coalesce with the other set of resonances; however this could not be demonstrated unambiguously because at these temperatures rapid decomposition of complex **11** severely hampers the interpretation of the ^1H NMR spectra.

The set of resonances of major intensity (cf. Table V) arises from the dynamic process depicted in Figure 4, which is fast on the NMR time scale at 283 K in C_6D_6.

Except for the ^{13}C resonances of the carbon atoms directly involved in the coordination changes, the remaining

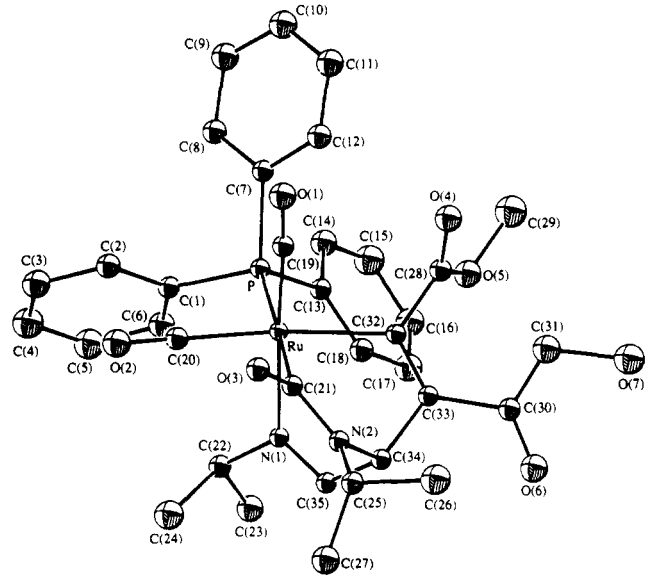

Figure 5. ORTEP diagram of complex **9b** showing 50% probability thermal elipsoids.

^{13}C and ^1H resonances appear roughly at the expected positions, analogous to those found for the $Fe(CO)_2$-(CNR)(THPP) complex. The three terminal carbonyl carbon atoms (C(1), C(2), C(3)) give rise to three separate resonances between 197 and 200 ppm. Whereas three of the four ester carbonyl carbon atoms resonate at normal positions (160–175 ppm), one of the ester carbonyl resonances is shifted downfield (197.4 ppm), which probably indicates that this carbonyl group is either in close proximity or even weakly coordinated to the metal during the dynamic process. The high field position (56–96 ppm) of all four resonances assigned to former alkyne carbon atoms (C(4), C(7), C(15), and C(18)), compared with those in the free THPP ligand (156.9 and 97.6 ppm), can be interpreted as the average of free and coordinated C=C resonances. When a solution of complex **11** in $CDCl_3$ is cooled to 243 K, broadening of all the resonances assigned to the exchanging isomers (both in the ^{13}C and the ^1H spectrum) is observed. On further cooling to 213 K the broadened resonances begin to sharpen up in two separate sets of resonances which indicates that the limit of slow exchange for the proposed dynamic process is well below 213 K. The dynamic behavior of $Ru(CO)_3$(THPP) in solution differs slightly from that of the analogous $Fe(CO)_2$(CN-*t*-Bu)-(THPP) complex.[31] The occurance of a σ-N,σ-N′-coordinated isomer (30%), which is absent in the iron complex, is probably related to the decreased affinity of ruthenium (compared with iron) for alkene π-coordination. The finding that the $Ru(CO)_3$ fragment migrates more readily from one ring of the THPP ligand to the other than the $Fe(CO)_2$CN-*t*-Bu fragment is probably related to the increased radius of the ruthenium atom and the absence of the sterically demanding CN-*t*-Bu ligand.

Molecular Structure of N(*i*-Pr)C(O)Ru(CO)$_2$-(PPh$_3$)C(CO$_2$Me)=C(CO$_2$Me)CHCH=N(*i*-Pr) (9b). The unit cell contains eight molecules of the complex and four tetrahydrofuran molecules of crystallization. An ORTEP drawing of the molecular geometry of **9b** together with the atomic numbering is shown in Figure 5. In

(29) Mann, B. E. *Adv. Organomet. Chem.* **1974**, *12*, 135.

(30) σ-N,σ-N′$Ru(CO)_3$THPP, ^1H NMR (300.13 MHz, 293 K, $CDCl_3$, δ (*J* in Hz)): for H(6), H(9), H(17), H(20) 3.82 (s, 6 H), 3.58 (s, 6 H); for H(13), H(14) 4.14 (s, 2 H); for H(10), H(21) 3.27 (sept, 6.5 Hz, 2 H); for H(11), H(12), H(22), H(23) ≈1.22–1.28 (m, partly obscured by the major set of resonances).

(31) Part VIII; de Lange, P. P. M.; Frühauf, H.-W.; van Wijnkoop, M.; Kraakman, M. J. A.; Kranenburg, M.; Groot, H. J. P.; Vrieze, K.; Fraanje, J.; Wang, Y.; Numan, M. To be published.

Table VI. Fractional Coordinates of the Non-Hydrogen Atoms and Equivalent Isotropic Thermal Parameters of Complex 9b

atom	x	y	z	U_{eq}, Å^2
Ru	0.11497 (1)	0.14899 (1)	0.10335 (2)	0.0290 (2)
C(1)	−0.0502 (2)	0.1135 (1)	0.2283 (3)	0.041 (2)
C(2)	−0.0841 (2)	0.1240 (1)	0.3304 (4)	0.058 (3)
C(3)	−0.1560 (3)	0.1353 (2)	0.3284 (6)	0.081 (4)
C(4)	−0.1938 (3)	0.1366 (2)	0.2284 (6)	0.081 (4)
C(5)	−0.1618 (3)	0.1252 (2)	0.1274 (5)	0.068 (3)
C(6)	−0.0902 (2)	0.1138 (1)	0.1261 (4)	0.050 (2)
C(7)	0.0436 (2)	0.0501 (1)	0.1730 (3)	0.040 (2)
C(8)	0.1073 (2)	0.0325 (1)	0.1397 (4)	0.053 (3)
C(9)	0.1104 (3)	−0.0069 (2)	0.1155 (4)	0.067 (3)
C(10)	0.0491 (4)	−0.0291 (1)	0.1244 (4)	0.072 (3)
C(11)	−0.0155 (3)	−0.0121 (1)	0.1543 (4)	0.067 (3)
C(12)	−0.0183 (2)	0.0275 (1)	0.1791 (4)	0.051 (2)
C(13)	0.0680 (2)	0.0947 (1)	0.3760 (3)	0.040 (2)
C(14)	0.0440 (3)	0.0626 (1)	0.4387 (4)	0.065 (3)
C(15)	0.0589 (4)	0.0590 (2)	0.5550 (4)	0.076 (3)
C(16)	0.0994 (3)	0.0871 (2)	0.6097 (4)	0.070 (3)
C(17)	0.1242 (3)	0.1182 (2)	0.5506 (4)	0.063 (3)
C(18)	0.1084 (2)	0.1221 (1)	0.4320 (4)	0.047 (2)
C(19)	0.1368 (2)	0.1122 (1)	−0.0114 (3)	0.041 (2)
C(20)	0.0335 (2)	0.1651 (1)	0.0130 (3)	0.041 (2)
C(21)	0.1711 (2)	0.1901 (1)	0.0021 (3)	0.036 (2)
C(22)	0.0293 (2)	0.2095 (1)	0.2667 (4)	0.045 (2)
C(23)	0.0302 (3)	0.2188 (2)	0.3963 (4)	0.064 (3)
C(24)	0.0046 (3)	0.2449 (2)	0.1981 (5)	0.079 (4)
C(25)	0.2584 (2)	0.2448 (1)	−0.0005 (4)	0.044 (2)
C(26)	0.3379 (3)	0.2382 (2)	0.0188 (6)	0.090 (4)
C(27)	0.2331 (3)	0.2846 (1)	0.0345 (5)	0.072 (3)
C(28)	0.2444 (2)	0.0996 (1)	0.2055 (4)	0.044 (2)
C(29)	0.2661 (4)	0.0508 (2)	0.3459 (7)	0.110 (5)
C(30)	0.3276 (2)	0.1702 (1)	0.2654 (3)	0.043 (2)
C(31)	0.4312 (3)	0.1337 (2)	0.3102 (6)	0.086 (4)
C(32)	0.2153 (2)	0.1392 (1)	0.1860 (3)	0.033 (2)
C(33)	0.2546 (2)	0.1701 (1)	0.2137 (3)	0.035 (2)
C(34)	0.2254 (2)	0.2101 (1)	0.1847 (3)	0.036 (2)
C(35)	0.1544 (2)	0.2184 (1)	0.2421 (3)	0.037 (2)
C(42)	0.2904 (8)	0.4762 (4)	0.2024 (11)	0.215 (13)
C(43)	0.2775 (6)	0.4852 (4)	0.3219 (9)	0.168 (10)
N(1)	0.1008 (2)	0.1965 (1)	0.2222 (3)	0.033 (2)
N(2)	0.2160 (2)	0.2146 (1)	0.0596 (3)	0.037 (2)
O(1)	0.1494 (2)	0.0918 (1)	−0.0865 (3)	0.066 (2)
O(2)	−0.0099 (2)	0.1754 (1)	−0.0486 (3)	0.069 (2)
O(3)	0.1638 (2)	0.1931 (1)	−0.1053 (2)	0.049 (2)
O(4)	0.2655 (2)	0.0782 (1)	0.1297 (3)	0.061 (2)
O(5)	0.2406 (2)	0.0896 (1)	0.3164 (3)	0.065 (2)
O(6)	0.3551 (2)	0.1987 (1)	0.3076 (3)	0.071 (2)
O(7)	0.3610 (2)	0.1364 (1)	0.2571 (4)	0.073 (2)
O(11)	0.2500 (0)	0.5000 (0)	0.1321 (11)	0.238 (15)
P	0.04523 (5)	0.10106 (2)	0.22219 (8)	0.0328 (4)

Tables VI and VII the atomic coordinates and selected bond lengths and angles are given. Molecules of **9b** have a [2.2.2] bicyclic structure in which the bridgehead positions are occupied by the ruthenium atom and the C—C-coupled former imine carbon atom. The coordination geometry around the central ruthenium atom is distorted octahedral with two terminal carbonyl ligands in a cis arrangement. The metal carbonyl bond Ru—C(20), trans to the vinylic C(32), is significantly longer than the Ru—C(19) bond which is positioned trans to the σ-donor N(1), reflecting better π-back-bonding in the latter direction. This arrangement is probably responsible for the very long Ru—C(32) bond of 2.131 (3) Å. The longest comparable Ru^{II}—C_{sp^2} bond distance found in the literature[20,32] measures 2.12 Å. The Ru—N(1) distance of 2.147 (3) Å is in agreement with values usually observed for Ru—N(imine) σ-bonds (between 2.10 and 2.15 Å).[33] As in the analogous

Table VII. Selected Bond Distances (Å) and Angles (deg) of the Non-Hydrogen Atoms of 9b (Esd's in Parentheses)

Ru–P	2.5071 (9)	N(1)–C(22)	1.500 (5)	C(33)–C(34)	1.515 (5)
Ru–C(19)	1.874 (4)	N(1)–C(35)	1.274 (5)	C(34)–C(35)	1.511 (5)
Ru–C(20)	1.927 (4)	N(2)–C(21)	1.361 (5)	C(32)–C(33)	1.329 (5)
Ru–C(21)	2.111 (4)	N(2)–C(34)	1.461 (5)		
Ru–C(32)	2.131 (3)	N(2)–C(25)	1.478 (5)		
Ru–N(1)	2.147 (3)	C(21)–O(3)	1.250 (4)		

P–Ru–C(19)	93.3 (1)	Ru–C(21)–O(3)	123.3 (3)
P–Ru–C(20)	94.2 (1)	N(2)–C(21)–O(3)	119.9 (3)
P–Ru–C(21)	178.5 (1)	C(23)–C(22)–C(24)	110.2 (4)
P–Ru–C(32)	96.3 (1)	C(23)–C(22)–N(1)	112.8 (3)
P–Ru–N(1)	94.91 (8)	C(24)–C(22)–N(1)	109.3 (3)
C(19)–Ru–C(20)	89.1 (2)	C(26)–C(25)–C(27)	113.9 (4)
C(19)–Ru–C(21)	87.2 (2)	C(26)–C(25)–N(2)	110.6 (4)
C(19)–Ru–C(32)	91.0 (1)	C(27)–C(25)–N(2)	110.1 (4)
C(19)–Ru–N(1)	171.7 (1)	Ru–C(32)–C(28)	122.4 (2)
C(20)–Ru–C(21)	84.4 (1)	Ru–C(32)–C(33)	117.9 (3)
C(20)–Ru–C(32)	169.5 (1)	C(28)–C(32)–C(33)	119.5 (3)
C(20)–Ru–N(1)	91.7 (1)	C(30)–C(33)–C(32)	127.2 (3)
C(21)–Ru–C(32)	85.1 (1)	C(30)–C(33)–C(34)	114.6 (3)
C(21)–Ru–N(1)	84.6 (1)	C(32)–C(33)–C(34)	118.1 (3)
C(32)–Ru–N(1)	86.7 (1)	C(33)–C(34)–C(35)	113.0 (3)
Ru–P–C(1)	112.0 (1)	C(33)–C(34)–N(2)	110.9 (3)
Ru–P–C(7)	117.7 (1)	C(35)–C(34)–N(2)	107.9 (3)
Ru–P–C(13)	119.0 (1)	C(34)–C(35)–N(1)	120.1 (3)
C(1)–P–C(7)	102.5 (2)	Ru–N(1)–C(22)	123.7 (2)
C(1)–P–C(13)	102.5 (2)	Ru–N(1)–C(35)	117.8 (2)
C(7)–P–C(13)	100.9 (2)	C(22)–N(1)–C(35)	117.7 (3)
Ru–C(19)–O(1)	175.4 (4)	C(21)–N(2)–C(25)	122.4 (3)
Ru–C(20)–O(2)	173.3 (4)	C(21)–N(2)–C(34)	119.3 (3)
Ru–C(21)–N(2)	116.8 (3)	C(25)–N(2)–C(34)	118.2 (3)

iron complexes,[3] the additional ligand, in this case PPh_3, is positioned trans to the inserted carbonyl ligand C(21)—O(3). The bond lengths in this Ru—C(=O)—N fragment show the same trend as in the analogous Fe—C(=O)—N fragment, a short C(21)—N(2) distance of 1.361 (5) Å indicating a partial double-bond character commonly found for amide functions[34] and a rather long Ru—C(21) bond of 2.111 (4) Å compared with $CpRu(CO)_2(CONH_2)$ (2.084 (7) Å).[35] Due to the C=C coupling the C(32)—C(33) bond (the former alkyne bond) is reduced to a double bond of 1.329 (5) Å, which is within the range found for this type of double bond,[36] and the former imine bond C(34)—N(2) is reduced to a single C—N bond of 1.461 (5) Å. The length of the newly formed C(33)—C(34) bond of 1.515 (5) Å is normal for a single bond. The relatively short C(35)—N(1) distance (1.274 (5) Å) of the intact imine fragment is caused by a decrease in π-back-donation into the C=N π* orbital, due to both the formally positively charged Ru atom and the increased energy level of this isolated π* orbital. It can be compared with the C=N distance in dinuclear C—C-coupled DAB complexes (i.e. $Ru_2(CO)_6$[AIB(*t*-Bu, CF_3, CF_3)][37] and $Ru_2(CO)_5$[AIP(*t*-Bu, *p*-Tol)][38]).

Molecular Structure of [NH(*i*-Pr)Ru(CO)$_3$C(CO$_2$Me)=C(CO$_2$Me)CHCH=N(*i*-Pr)]$^+$BF$_4^-$ (10). An ORTEP drawing of the molecular structure of **10** together with the atomic numbering is shown in Figure 6.

(32) Tables of Ru–C bond lengths can be found in: (a) Wisner, J. M.; Bartczak, T. J.; Ibers, J. A. *Inorg. Chim. Acta* **1985**, *100*, 115. (b) Bruce, M. I. *Pure Appl. Chem.* **1986**, *58*, 553.

(33) Polm, L. H.; Mul, W. P.; Elsevier, C. J.; Vrieze, K.; Christophersen, M. J. N.; Stam, C. H. *Organometallics* **1988**, *7*, 423. See also refs 8 and 37.

(34) *Handbook of Chemistry and Physics*, 56th ed., CRC Press: Cleveland, OH, **1975**.

(35) Wagner, H.; Jungbauer, A.; Thiele, G.; Behrens, H. *Z. Naturforsch.* **1979**, *34B*, 1487.

(36) Hoffmann, K.; Weiss, E. *J. Organomet. Chem.* **1977**, *128*, 399. See also ref 20.

(37) Muller, F.; Dijkhuis, D. I. P.; van Koten, G.; Vrieze, K.; Heijdenrijk, D.; Rotteveel, M. A.; Stam, C. H.; Zoutberg, M. C. *Organometallics* **1989**, *8*, 992.

(38) Keijsper, J.; Polm, L. H.; van Koten, G.; Vrieze, K.; Stam, C. H.; Schagen, J.-D. *Inorg. Chim. Acta* **1985**, *103*, 137.

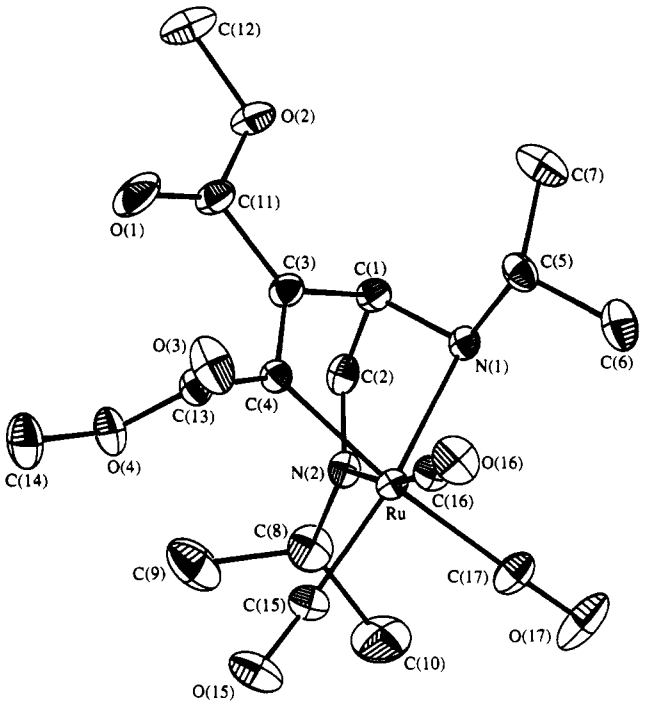

Figure 6. ORTEP diagram of complex **10** showing 50% probability thermal elipsoids.

Table VIII. Fractional Coordinates of the Non-Hydrogen Atoms and Equivalent Isotropic Thermal Parameters of 10

atom	*x*	*y*	*z*	U_{eq}, Å^2
Ru	0.21796 (2)	0.44399 (2)	0.17612 (1)	0.0370 (2)
C(1)	0.1242 (3)	0.3873 (3)	0.0655 (2)	0.046 (2)
C(2)	0.1109 (3)	0.4743 (3)	0.0605 (2)	0.049 (2)
C(3)	0.2322 (3)	0.3712 (3)	0.0517 (2)	0.047 (2)
C(4)	0.2942 (3)	0.3964 (2)	0.0975 (2)	0.041 (2)
C(5)	0.1026 (3)	0.2829 (3)	0.1520 (3)	0.054 (3)
C(6)	0.0351 (5)	0.2384 (4)	0.1054 (4)	0.089 (4)
C(7)	0.0685 (4)	0.2739 (3)	0.2217 (3)	0.075 (4)
C(8)	0.1382 (5)	0.6018 (3)	0.1002 (3)	0.076 (4)
C(9)	0.2303 (6)	0.6309 (4)	0.0659 (4)	0.109 (6)
C(10)	0.1064 (7)	0.6377 (4)	0.1622 (4)	0.114 (6)
C(11)	0.2632 (4)	0.3337 (3)	−0.0105 (2)	0.058 (3)
C(12)	0.2088 (6)	0.2686 (5)	−0.1047 (3)	0.104 (5)
C(13)	0.4031 (3)	0.3847 (3)	0.0951 (2)	0.048 (2)
C(14)	0.5561 (4)	0.4364 (4)	0.0622 (4)	0.085 (4)
C(15)	0.3183 (4)	0.5174 (3)	0.1972 (2)	0.053 (3)
C(16)	0.2796 (3)	0.3655 (3)	0.2289 (2)	0.049 (2)
C(17)	0.1299 (4)	0.4816 (3)	0.2476 (2)	0.063 (3)
N(1)	0.1073 (2)	0.3689 (2)	0.1354 (2)	0.041 (2)
N(2)	0.1475 (3)	0.5157 (2)	0.1058 (2)	0.044 (2)
O(1)	0.3472 (3)	0.3287 (4)	−0.0276 (2)	0.111 (4)
O(2)	0.1871 (3)	0.3045 (2)	−0.0421 (2)	0.065 (2)
O(3)	0.4439 (3)	0.3297 (2)	0.1187 (2)	0.086 (3)
O(4)	0.4485 (2)	0.4447 (2)	0.0691 (2)	0.063 (2)
O(15)	0.3788 (3)	0.5613 (2)	0.2080 (2)	0.082 (3)
O(16)	0.3135 (3)	0.3164 (2)	0.2575 (2)	0.075 (2)
O(17)	0.0823 (4)	0.5003 (4)	0.2885 (2)	0.110 (4)
B	0.3628 (5)	0.4675 (4)	0.3746 (3)	0.070 (4)
F(1)	0.2729 (3)	0.4514 (5)	0.3574 (3)	0.173 (6)
F(2)	0.3973 (4)	0.4175 (4)	0.4221 (2)	0.134 (4)
F(3)	0.4276 (3)	0.4548 (2)	0.3220 (2)	0.083 (2)
F(4)	0.3815 (6)	0.5359 (3)	0.4048 (3)	0.174 (5)

In Tables VIII and IX the atomic coordinates and selected bond lengths and angles are given. Molecules of **10** consist of an anionic BF_4 unit and a cationic Ru complex which has a [2.2.1]bicyclic structure with the ruthenium atom and the former imine carbon atom occupying the bridgehead positions. The coordination geometry around the central ruthenium atom is distorted octahedral. As a consequence of its [2.2.1] bicyclic structure, the newly formed tridentate ligand is not able to span three regular octahedral positions. This is reflected in the N(1)—Ru—N(2), C(4)—Ru—N(1), and C(4)—Ru—N(2) angles of 76.3 (1), 78.9 (1), and 85.2 (1)°, respectively, values that were also observed in a comparable iron complex.[6] The remaining angles around the ruthenium atom are consequently larger than 90°. The rather long Ru—C(17) bond of 2.003 (5) Å compared with Ru—C(15) (1.899 (5) Å) and Ru—C(16) (1.920 (5) Å) can be explained by the large trans influence of C(4), which tends to elongate this bond, and the comparatively smaller trans influence of N(1) and N(2) on the latter bond distances. The Ru—C(4) distance of 2.088 (4) Å is within the range of 2.02—2.09 Å typically found for Ru—C_{sp^2} bonds.[32] The intact imine fragment C(2)—N(2) (1.272 (6) Å) is σ-N-coordinated to Ru by a normal σ-donative bond of 2.216 (3) Å. The geometry around the amine N(1) is distorted tetrahedral with the *i*-Pr group slightly bent away from the metal (Ru—N(1)—C(5) 121.6 (3)°). Both the former imine C(1)—N(1) and the C(5)—N(1) distances of 1.494 (5) and 1.509 (6) Å, respectively, are normal for a C—N single bond. The other distances in the carbon backbone of the [2.2.1] bicyclic moiety, the newly formed C(1)—C(3) single bond of 1.514 (6) Å and a double bond of 1.336 (6) Å between C(3) and C(4), closely resemble those in complex **9b**.

Table IX. Selected Bond Distances (Å) and Angles (deg) of the Non-Hydrogen Atoms of 10 (Esd's in Parentheses)

Ru–C(4)	2.088 (4)	N(1)–C(5)	1.509 (6)	C(4)–C(13)	1.487 (6)
Ru–C(15)	1.899 (5)	N(2)–C(2)	1.272 (6)	C(15)–O(15)	1.133 (6)
Ru–C(16)	1.920 (5)	N(2)–C(8)	1.483 (6)	C(16)–O(16)	1.123 (6)
Ru–C(17)	2.003 (5)	C(1)–C(2)	1.502 (7)	C(17)–O(17)	1.109 (7)
Ru–N(1)	2.144 (3)	C(1)–C(3)	1.514 (6)		
Ru–N(2)	2.126 (3)	C(3)–C(4)	1.336 (6)		
N(1)–C(1)	1.494 (5)	C(3)–C(11)	1.495 (7)		

C(4)–Ru–C(15)	94.7 (2)	C(3)–C(4)–C(13)	123.7 (4)
C(4)–Ru–C(16)	87.4 (2)	C(6)–C(5)–C(7)	111.3 (4)
C(4)–Ru–C(17)	172.6 (2)	C(6)–C(5)–N(1)	111.6 (4)
C(4)–Ru–N(1)	78.9 (1)	C(7)–C(5)–N(1)	109.1 (4)
C(4)–Ru–N(2)	85.2 (1)	C(9)–C(8)–C(10)	120.3 (6)
C(15)–Ru–C(16)	91.2 (2)	C(9)–C(8)–N(2)	106.9 (5)
C(15)–Ru–C(17)	92.5 (2)	C(10)–C(8)–N(2)	111.6 (5)
C(15)–Ru–N(1)	170.0 (2)	C(3)–C(11)–O(1)	123.5 (5)
C(15)–Ru–N(2)	95.6 (2)	C(3)–C(11)–O(2)	111.6 (4)
C(16)–Ru–C(17)	93.7 (2)	O(1)–C(11)–O(2)	124.9 (5)
C(16)–Ru–N(1)	96.2 (2)	C(4)–C(13)–O(3)	123.4 (4)
C(16)–Ru–N(2)	170.3 (2)	C(4)–C(13)–O(4)	112.0 (4)
C(17)–Ru–N(1)	93.8 (2)	O(3)–C(13)–O(4)	124.4 (4)
C(17)–Ru–N(2)	92.9 (2)	Ru–C(15)–O(15)	178.0 (5)
N(1)–Ru–N(2)	76.3 (1)	Ru–C(16)–O(16)	176.0 (4)
C(2)–C(1)–C(3)	106.4 (3)	Ru–C(17)–O(17)	177.5 (5)
C(2)–C(1)–N(1)	104.8 (3)	Ru–N(1)–C(1)	98.4 (2)
C(3)–C(1)–N(1)	106.9 (3)	Ru–N(1)–C(5)	121.6 (3)
C(1)–C(2)–N(2)	117.0 (4)	C(1)–N(1)–C(5)	115.4 (3)
C(1)–C(3)–C(4)	114.5 (4)	Ru–N(2)–C(2)	110.9 (3)
C(1)–C(3)–C(11)	120.7 (4)	Ru–N(2)–C(8)	131.6 (3)
C(4)–C(3)–C(11)	124.8 (4)	C(2)–N(2)–C(8)	117.5 (4)
Ru–C(4)–C(3)	111.5 (3)	C(11)–O(2)–C(12)	116.1 (5)
Ru–C(4)–C(13)	124.6 (3)	C(13)–O(4)–C(14)	115.4 (4)

Conclusions

The reaction of $Ru(CO)_3$(*i*-Pr-DAB) with the activated alkyne DMADC results in formation of the different bicyclic products described in this article and depends on the additional ligand offered. In comparison to the analogous $Fe(CO)_3$(R-DAB) complexes the activation energy for the initial 1,3-dipolar cycloaddition is lower, whereas the following intermediates show an increase in stability. This enabled us to obtain more information on the mechanistic details governing the reactions of M-$(CO)_3$(R-DAB) complexes with activated alkynes and to firmly establish the 1,3-dipolar cycloaddition mechanism as the initial reaction step. Mechanistic understanding is crucial for an extension of the scope of this type of reaction

that produces synthetically interesting, highly functionalized organic heterocycles.

Acknowledgment. We thank J. Fraanje and D. J. A. De Ridder for collecting the X-ray data, M. J. A. Kraakman for helpful discussions, and J.-M. Ernsting for this advice on recording the 300.13-MHz heteronuclear 2D-correlated NMR spectra.

Supplementary Material Available: Tables of fractional coordinates and isotropic thermal parameters of the hydrogen atoms, anisotropic thermal parameters, and complete bond distances and angles of both the hydrogen and non-hydrogen atoms of complexes **9b** and **10** (12 pages). Ordering information is given on any current masthead page.

OM920175K

Open and Half-Open Manganocene Chemistry: More Associated Salts

Michael S. Kralik,[1a] Lothar Stahl,[1a] Atta M. Arif,[1a] Charles E. Strouse,[1b] and Richard D. Ernst*,[1a]

Departments of Chemistry, University of Utah, Salt Lake City, Utah 84112, and University of California, Los Angeles, California 90024

Received May 14, 1992

The reaction of $MnCl_2$ with 1 equiv each of NaC_5H_5 and $K(2,4\text{-}C_7H_{11})$ (C_7H_{11} = dimethylpentadienyl) leads to $Mn_2(C_5H_5)_2(2,4\text{-}C_7H_{11})$. This species may be considered to be an associated salt of high-spin $Mn(C_5H_5)^+$ and the 18-electron $Mn(C_5H_5)(2,4\text{-}C_7H_{11})^-$. In accord with this, magnetic susceptibility measurements demonstrate the presence of five unpaired electrons. A single-crystal X-ray diffraction study has been undertaken. The space group is $P2_1/m$ with a = 7.495 (2), b = 12.500 (7), c = 8.678 (3) Å, β = 106.88 (2)°, and V = 778.0 Å^3, for Z = 2. The structure has been refined to discrepancy indexes of R = 0.075 and R_w = 0.078. The reaction of $MnCl_2$ with 2 equiv of $K[3\text{-}CH_3\text{-}1,5\text{-}(Me_3Si)_2C_5H_4]$ also leads to an associated salt, $K\{Mn[3\text{-}CH_3\text{-}1,5\text{-}(Me_3Si)_2C_5H_4]_3\}$, again with high-spin Mn^{2+} (five unpaired electrons). An X-ray diffraction study revealed that the Mn^{2+} center experiences trigonal planar coordination with the three η^1-bound dienyl ligands, while K^+ is encapsulated within the three dienyl chains. The space group at −140° is *Pcab* (No. 61), with a = 19.180 (4), b = 26.895 (4), c = 18.843 (5) Å, and V = 9720.1 Å^3 for Z = 8. The structure has been refined to discrepancy indexes of R = 0.068 and R_w = 0.068.

While bis(cyclopentadienyl)metal complexes, the metallocenes, have been known for some time, it has only been fairly recently that a series of "open metallocenes", or bis(pentadienyl)metal complexes, has been reported.[2] Such complexes are now known for titanium, zirconium, vanadium, chromium, iron, ruthenium, and osmium and have provided for some interesting structural and reactivity comparisons between the two series. It is important to note that the behavior of manganese in each series is quite anomalous. For example, manganocene's chemical behavior is generally regarded as highly ionic, and a polymeric structure has been determined in the solid state, although the high-spin monomeric species is present in the gas phase. Conversion to a low-spin form may be brought about by the introduction of methyl groups onto the rings.[3] In contrast, attempts to prepare a bis(3-methylpentadienyl)manganese complex, $Mn(3\text{-}C_6H_9)_2$, led instead to an unusual $Mn_3(3\text{-}C_6H_9)_4$ species, which was initially formulated as an associated salt of high-spin Mn^{2+} and two diamagnetic $Mn(3\text{-}C_6H_9)_2^-$ units.[4] It was believed that the reaction did indeed first lead to an "open manganocene" but that some of these species underwent an intramolecular coupling reaction, leading to a methylpentadienyl dimer which was subsequently replaced from the manganese atom by two $Mn(3\text{-}C_6H_9)_2$ units, forming the observed trimetallic product. Since this unexpected reaction prevented study of a true "open manganocene", alternative approaches must be considered. For example, a half-open manganocene such as $Mn(C_5H_5)(2,4\text{-}C_7H_{11})$ (C_7H_{11} = dimethylpentadienyl) might be more feasible. In such a complex, a coupling reaction between pentadienyl ligands should be less favorable and would have to take place intermolecularly. Alternatively, preparation of an open manganocene might be possible if the sites most prone to undergoing coupling reactions were sterically blocked by appropriate substituents. In the hope of obtaining some information about the open and half-open manganocenes, we have attempted the preparations of $Mn(C_5H_5)(2,4\text{-}C_7H_{11})$ and $Mn[3\text{-}CH_3\text{-}1,5\text{-}(Me_3Si)_2C_5H_4]_2$. In fact, once again more complex associated salt species have been isolated. Herein we describe the nature of the complex products, $Mn_2(C_5H_5)_2(2,4\text{-}C_7H_{11})$ and $KMn[3\text{-}CH_3\text{-}1,5\text{-}(Me_3Si)_2C_5H_4]_3$.

Experimental Section

All procedures were carried out under a nitrogen atmosphere, and all solvents were dried by treatment with Na/K and benzophenone and distilled under a nitrogen atmosphere. Elemental analyses were carried out by Analytische Laboratorien (Gummersbach) and Beller Mikroanalytisches Laboratorium (Göttingen).

(2,4-Dimethylpentadienyl)bis(cyclopentadienyl)dimanganese, $Mn_2(C_5H_5)_2(2,4\text{-}C_7H_{11})$. A stirred suspension of 1.00 g (8.0 mmol) of manganous chloride in 50 mL of THF was cooled to −78 °C. To this slurry was added dropwise a mixture of 1.07 g (8.0 mmol) of potassium 2,4-dimethylpentadienide and 0.70 g (8.0 mmol) of sodium cyclopentadienide dissolved in 50 mL of THF. The resulting solution was allowed to warm slowly to room temperature, after which stirring was continued for another 4 h. At this time, the solvent was removed in vacuo, and the product was extracted with three 20-mL portions of hexane and filtered

(1) (a) University of Utah. (b) University of California.
(2) Ernst, R. D. *Chem. Rev.* **1988**, *88*, 1255.
(3) (a) Evans, S.; Green, M. L. H.; Jewitt, B.; Orchard, A. F.; Pygall, C. F. *J. Chem. Soc., Faraday Trans. 2* **1972**, *68*, 1235. (b) Almenningen, A.; Haaland, A.; Samdal, S. *J. Organomet. Chem.* **1978**, *149*, 219. (c) Bünder, W.; Weiss, E. *Z. Naturforsch.* **1978**, *33B*, 1235. (d) Freyberg, D. P.; Robbins, J. L.; Raymond, K. N.; Smart, J. C. *J. Am. Chem. Soc.* **1979**, *101*, 892.
(4) Böhm, M. C.; Ernst, R. D.; Gleiter, R.; Wilson, D. R. *Inorg. Chem.* **1983**, *22*, 3815.

0276-7333/92/2311-3617$03.00/0